UNIVERSITY OF AMSTERDAM

UvA-DARE (Digital Academic Repository)

A Stable Aminyl Radical Coordinated to Cobalt

Rodríguez-Lugo, R.E.; de Bruin, B.; Trincado, M.; Grützmacher, H.

Link to publication

▌**Coordination Chemistry** |*Hot Paper*|

A Stable Aminyl Radical Coordinated to Cobalt

Rafael E. Rodríguez-Lugo,[a, b, c] Bas de Bruin,*[d] Monica Trincado,*[a] and Hansjörg Grützmacher*[a]

Dedicated to Professor Karl Wieghardt on the occasion of his 75th birthday

Abstract: A family of cobalt complexes bearing the trop$_2$NH [bis(5-*H*-dibenzo[*a,d*]cyclohepten-5-yl)-amine] and 2,2′-bpy (2,2′-bipyridine) chelate ligands were prepared and fully characterized. The compounds [Co(trop$_2$N)(bpy)], [Co(trop$_2$NH)(bpy)]$^+$, and [Co(trop$_2$N)(bpy)]$^+$ are cobalt complexes interrelated by one-electron redox processes and/or proton transfer. Two limiting resonance structures can be used to describe the paramagnetic complex [Co(trop$_2$N)(bpy)]$^+$: [Co^{II}(trop$_2$N$^-$)(bpy)]$^+$ (Co^{II} amido) and [Co^I(trop$_2$N$^.$)(bpy)]$^+$ (Co^I-aminyl radical). Structural data, DFT calculations, and reactivity toward H-abstraction indicate a slightly higher contribution of the aminyl radical form to the ground state of [Co(trop$_2$N)(bpy)]$^+$. The results described here complete the series of Group 9 metal aminyl radical complexes bearing the diolefin amine ligand trop$_2$NH.

Introduction

Metalloradicals are compounds in which the spin density is significantly confined to the metal center. Nevertheless, there are cases in which the unpaired electron can be delocalized onto the ligand or is significantly localized there.[1] There are well-defined examples of metal coordinated phenoxyl,[2] tyrosyl,[2] verdazyl,[3] thiazyl,[4] and nitrogen-centered radical ligands.[5] Organic compounds with open-shell *N*-donors are highly reactive short-lived species in their free form,[6] and coordination to a metal fragment is actually a way to make them more persistent and even isolable. In the past few years, examples of metal complexes with aminyl ($^.$NR$_2$), nitrene radical/imidyl ($^.$NR), and nitridyl radical ligands ($^.$N) have been isolated, and despite their intrinsic high reactivity, they have demonstrated high selectivity in certain catalytic processes.[5] Warren and co-

workers isolated and characterized the nickel(II) imidyl radical complex **A** (Figure 1).[7] Related and catalytically relevant imidyl/nitrene radical complexes of cobalt porphyrins (**B**) were characterized in detail by de Bruin and co-workers using a variety of spectroscopic (EPR, X-ray absorption, UV/Vis, IR), compu-
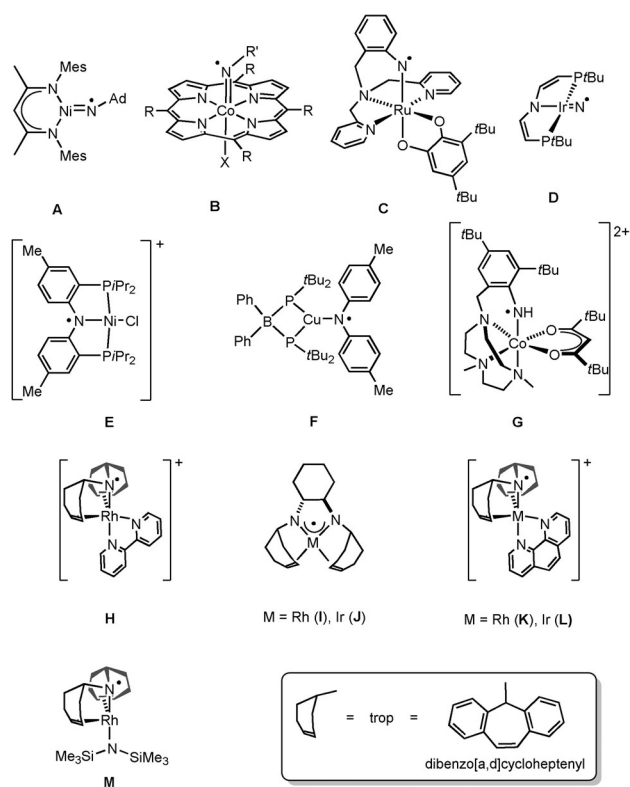
[a] *Dr. R. E. Rodríguez-Lugo, Dr. M. Trincado, Prof. Dr. H. Grützmacher*
Department of Chemistry and Applied Biosciences
Eidgenössische Technische Hochschule Zürich
Vladimir-Prelog-Weg 1–5/10, 8093 Zürich (Switzerland)
E-mail: trincado@inorg.chem.ethz.ch
        hgruetzmacher@ethz.ch

[b] *Dr. R. E. Rodríguez-Lugo*
Current address: Centro de Química
Instituto Venezolano de Investigaciones Científicas (IVIC)
Altos de Pipe, 1020-A Caracas (Venezuela)

[c] *Dr. R. E. Rodríguez-Lugo*
Current address: Departamento de Química
Universidad Simón Bolívar (USB)
Valle de Sartenejas, 1080-A Caracas (Venezuela)

[d] *Prof. Dr. B. de Bruin*
Van't Hoff Institute for Molecular Sciences, Universiteit van Amsterdam
Science Park 904, 1098 XH Amsterdam (The Netherlands)
E-mail: b.debruin@uva.nl

📄 *Supporting information and the ORCID numbers for the authors of this*
article can be found under http://dx.doi.org/10.1002/chem.201605624.

Figure 1. Selected examples of imidyl (**A**–**C**),[7,8,15] nitridyl (**D**),[16] and aminyl (**E**–**M**)[21–31] radical complexes.

tational, and mass spectrometric techniques.[8] Other imidyl radical (˙NR) complexes have also been described by Wieghardt,[9] Peters,[10] Chirik,[11] Holland,[12] Caulton,[13] and Betley.[14] The ruthenium(II)-semiquinone-anilino radical **C** was prepared by Tanaka and co-workers.[15] Mindiola reported the first parent Ti-imido complex formed using a radical nitridyl species.[16a] The groups of Schneider and de Bruin detected spectroscopically for the first time a transient "nitridyl" radical complex (Ir≡N˙) **D** [IrN(L^{tBu})] [L^{tBu} = N(CHCHP-tBu$_2$)$_2$].[16b,c] An analogous transient Rh≡N˙ nitridyl complex was also spectroscopically detected.[17] More recently, the same groups reported the isolation and structural characterization of a bridging [(PNN)Rh{N˙}Rh(PNN)] nitridyl radical complex (PNN = 6-di-(tert-butyl)phosphinomethyl-2,2′-bipyridine).[18] Early examples of metal aminyl radical compounds were proven incorrect.[19,20] These complexes were difficult to classify because two limiting resonance structures, [M^{+}]—($^{-}$NR$_2$) (metal amide) or [M]—(˙NR$_2$) (aminyl radical complex), can be formulated.

Nowadays, the combination of spectroscopic data with high-level computational studies can help to address the location of the unpaired electron in the metallic fragment. Selected examples of aminyl radical (˙NR$_2$) complexes are shown in Figure 1 (**E**–**M**).[21–31] N-containing pincer ligands have been employed frequently to stabilize aminyl radical ligands. For example, Mindiola and co-workers fully characterized the nickel(II)-PNP complex **E**, with 69% of the spin density spread over the aminyl pincer moiety (32% on the nitrogen atom, 37% on the aromatic rings).[21] Nocera extended this study to Mn and Re complexes,[22] and Peters synthesized a copper(I)-bis-(aminyl) species.[23] More recently, the same authors isolated a copper(I) aminyl radical complex **F**, bearing a non-chelating ligand.[24] A related example with a NacNac ligand was reported by Warren and co-workers.[25] Wieghardt and co-workers reported the cobalt(III)-aniline radical complex **G**.[26] Our group described the first well defined example of a stable aminyl radical coordinated to a metal (complex **H**), in which DFT calculations indicate that approximately 54% of the total spin density was located on the nitrogen atom and about 30% on the metal atom.[27] For the diolefin diaminyl complex **I**, the spin population estimated experimentally by analysis of the EPR hyperfine interactions indicates that about 56% of the spin is delocalized and spread over the two nitrogen atoms.[28] These studies were extended to iridium(I) complexes **J**[29] and **L**.[30] Remarkably, the iridium compound **J** is an efficient catalyst for the chemoselective oxidation of primary alcohols to aldehydes.[29] For **H**, **I**, **K**, and **L**, reactivity studies towards H-atom abstraction using XH reagents (X = R$_3$Sn, RS, RO, R$_3$Si, R$_3$C) were carried out, which confirmed ligand-centered reactivity.[27,28,30] More recently, the oxidation of an anionic diamido Rh^{I} complex resulted in a delocalized metallo-amine radical with evenly distributed spin population on both the metal and ligand (**M**).[31] With exception of complexes **H**—**M**, only a recent example from Cundari and co-workers has been reported describing an aminyl radical ligand with a non-conju-

gated substituent on the N-atom, in which the spin density can be additionally delocalized.[32] Here, we report the first stable aminyl radical complex of cobalt. A comparison of its spectroscopic properties, electrochemical behavior, spin density, structural features, and reactivity with respect to the heavier Rh and Ir analogues is made.[27,30] These results complete the trop-series of "metal aminyl radical complexes of Group 9", and extends our understanding of the chemistry of the [M(trop$_2$NH)(bpy)]$^{+}$ (M = Co, Rh, Ir) series.

Results and Discussion

The complex [Co(trop$_2$N)(bpy)] (**1**) can be obtained directly by mixing equimolar amounts of [Co(HMDS)$_2$], trop$_2$NH and 2,2′-bipyridine (bpy) in presence of an excess of Zn powder as a reducing agent (Scheme 1). Deep-red crystals are obtained in
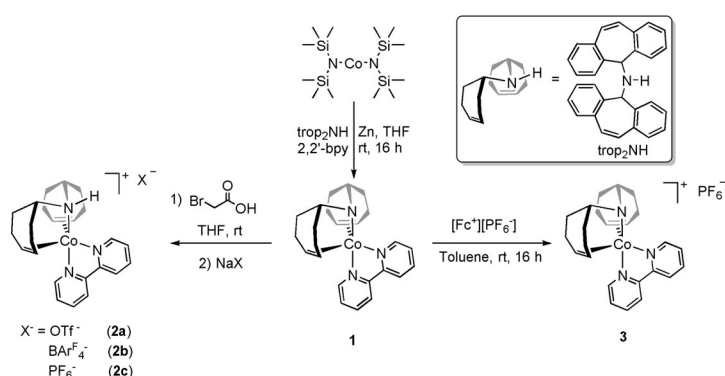
Scheme 1. Synthesis of amido, amino, and aminyl cobalt complexes **1**, **2**, and **3** (OTf^{-} = trifluoromethanesulfonate, BAr$^{F}_4{}^{-}$ = tetrakis[3,5-bis(trifluoromethyl)phenyl]borate).

70% yield upon layering a THF solution of the complex with n-hexane. The amido cobalt(I) complex **1** can be quantitatively protonated using 2-bromoacetic acid (pK$_a$ = 2.86 in H$_2$O). Upon protonation, salt metathesis with NaX (X^{-} = OTf^{-}, BAr$^{F}_4{}^{-}$, PF$_6{}^{-}$) leads to the formation of complexes **2** [X = OTf^{-} (**2a**), BAr$^{F}_4{}^{-}$ (**2b**), PF$_6{}^{-}$ (**2c**)]. Orange single crystals of complex **2c** suitable for X-ray diffraction analysis were isolated in good yield (60%). Chemical oxidation of amido complex **1** with ferrocenium hexafluorophosphate [Fc^{+}][PF$_6{}^{-}$] in toluene resulted in precipitation of the green complex **3**. Pale green single crystals of **3** were obtained from a dichloromethane solution.

Selected ^{13}C and ^{1}H NMR spectroscopic data of the diamagnetic complexes **1** and **2a** are listed in Table 1. The corresponding data for the previously reported analogous complexes [Rh(trop$_2$N)(bpy)] (**4**), [Rh(trop$_2$NH)(bpy)]OTf (**5**), [Ir(trop$_2$N)(phen)] (**6**), and [Ir(trop$_2$NH)(phen)]PF$_6$ (**7**) (phen = 1,10-phenanthroline) are also shown for comparison.[27,30] On comparing the neutral amido species [M(trop$_2$N)(bpy)] (M = Co, Rh, Ir) with the cationic amine species [M(trop$_2$NH)(bpy)]$^{+}$, it is clear that the ^{1}H and ^{13}C NMR resonances assigned to the coordinated CH=CH$_{trop}$ signals are shifted in all cases to higher frequencies upon protonation of the amido moiety. Both the missing positive charge and the increased electron donation of

Table 1. Selected ^{13}C and ^{1}H NMR spectroscopic data of complexes **1**, **2a**, and **4–7**.[27,30] Chemical shifts are given on the δ scale in ppm. All data were obtained in [D$_8$]THF unless otherwise stated.

Complex	δ olefinic H^a/H^b ($^3J_{HH}$ [Hz])	δ olefinic C^a/C^b	δ NH
1, [Co(trop$_2$N)(bpy)]	3.96/5.38 (9.4)	71.2/73.5	–
2a, [Co(trop$_2$NH)(bpy)]OTf	4.79/6.21 (9.5)	75.6/75.7	0.86
4,[a] [Rh(trop$_2$N)(bpy)]	3.42 (9.1)/4.84 (9.3)	64.1/65.7	–
5,[b] [Rh(trop$_2$NH)(bpy)]OTf	3.95/5.22 (9.3)	68.8/69.7	3.72
6, [Ir(trop$_2$N)(phen)]	2.72 (8.8)/4.81 (9.1)	44.0/50.8	–
7, [Ir(trop$_2$NH)(phen)]PF$_6$	3.26 (8.8)/5.18 (9.3)	47.9/51.1	4.78

[a] In [D$_6$]DMSO. [b] In CDCl$_3$.

the amido group places more electron density on the metal center, which leads to enhanced π-back donation to the olefinic trop moieties, thus shielding their resonances. As expected, this M→(C=C$_{trop}$) back donation increases from Co to Ir and the CH=CH$_{trop}$ signals (^1H and ^{13}C NMR spectra) are shifted to lower frequencies indicating increased shielding. The opposite effect is seen for the NH resonances. The more electron-rich metal complexes (Ir > Rh > Co) exhibit more deshielded NH signals, which is most likely a consequence of greater π-back-bonding from the metal to the olefinic moieties (CH=CH$_{trop}$). As a consequence, the NH function is significantly more acidic in the Rh [pK_a^{DMSO} = 18.7(2)] and Ir complexes [pK_a^{DMSO} = 18.2(2)] than in the cobalt complex.[30]

The redox properties of **1** were studied electrochemically by cyclic voltammetry (Figure 2). The results are summarized in Table 2. The redox potentials for **4**[27] and **6**[30] are also presented for comparison. The cyclic voltammogram of the neutral co-
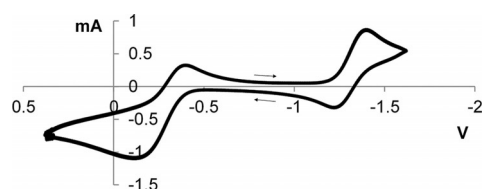
Figure 2. Cyclic voltammetry of **1** in THF containing 0.1 M nBu$_4$N$^+$PF$_6^-$. Scan rate 100 mV s^{-1}, scan range between +1 to −1 V (0.38 to −1.62 V vs. Fc/Fc$^+$ couple).

Table 2. Redox potential for complexes **1**, **4**,[27] and **6**[30] referenced against Fc/Fc$^+$ couple.

Complex	$E^\circ_{1/2}$ [V]	Redox behavior
1,[a] [Co(trop$_2$N)(bpy)]	−0.26, −1.31	quasi-reversible
4,[b] [Rh(trop$_2$N)(bpy)]	−0.55	reversible
6,[b] [Ir(trop$_2$N)(phen)]	−0.60	reversible

[a] In THF. [b] In DMSO.

balt(I) amido complex **1** shows two quasi-reversible redox waves at $E^1_{1/2}$ = −0.26 V and $E^2_{1/2}$ = −1.31 V (vs. Fc/Fc$^+$), respectively (Figure 2). The redox waves are assigned to the couples [Co(trop$_2$N)(bpy)]$^{2+}$/[Co(trop$_2$N)(bpy)]$^+$ ($E^1_{1/2}$ = −0.26 V) and

[Co(trop$_2$N)(bpy)]$^+$/[Co(trop$_2$N)(bpy)] ($E^2_{1/2}$ = −1.31 V). In contrast, the heavier analogues of **1** exhibit one reversible redox wave within the same voltage range.[27,30] The values listed in Table 2 show that [Co(trop$_2$N)(bpy)] is oxidized at a significantly lower potential than [Rh(trop$_2$N)(bpy)] or [Ir(trop$_2$N)(phen)].

The structures of **1**, **2c**, and **3** were determined by X-ray diffraction studies and are shown in Figures 3–5, respectively. Selected bond distances and angles are listed in Table 3. The corresponding data for the analogous complexes
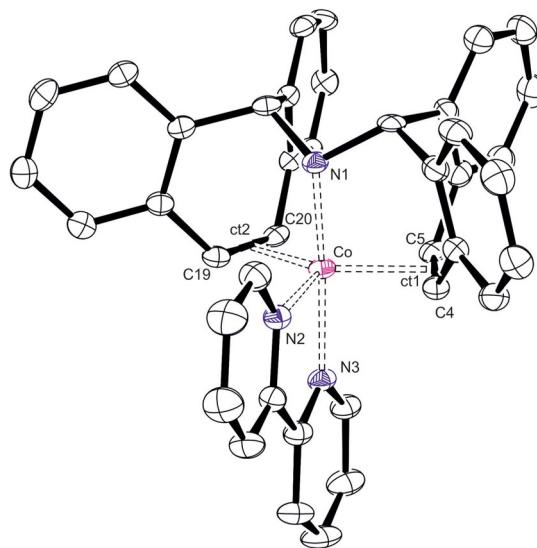
Figure 3. ORTEP drawing of the molecular structure of **1**. Thermal ellipsoids are drawn at 50% probability level. Non-relevant hydrogen atoms and a hexane solvate molecule have been removed for clarity. ct is the centroid of the coordinated C4=C5 and C19=C20 bonds, respectively. Two independent molecules per unit cell were found. The values reported for selected bond distances and angles correspond to the average. Selected bond distances [Å] and angles [°]: Co−N1 1.954(2), Co−N2 2.004(3), Co−N3 1.991(2), C4−C5 1.429(4), C19−C20 1.416(4), Co−ct1 1.921(3), Co−ct2 1.923(3); N1-Co-N3 171.7(1), ct1-Co-ct2 135.6(1), N1-Co-N2 91.6(1); Σ° N1 343.6(2).

[Rh(trop$_2$N)(bpy)] (**4**), [Rh(trop$_2$NH)(bpy)]OTf (**5**), and [Rh(trop$_2$N)(bpy)]OTf (**8**) are shown for comparison.[27] In the three complexes, the cobalt centers reside in distorted trigonal bipyramidal (TBP) coordination spheres with the largest deviation seen in the ct1-Co-ct2 angles (ct is the centroid of the coordinated double bonds), which varies between 135°–143° (ideally 120°). Significant structural changes occur when the neutral amido complex **1** is oxidized to the radical cation complex **3** (Table 3). The Co−N1 bond [1.954(2) vs. 1.842(2) Å] is shortened, the N1-Co-N3 angle [171.7(1)° vs. 178.7(1)°] becomes closer to 180° and the arrangement of the substituents on the N1 center flattens [Σ° N1 = 343.6(2)° vs. Σ° N1 = 358.4(3)°], which indicates that the electron is removed from a Co−N1 π-antibonding orbital. Similar structure alterations were observed when the neutral rhodium complex **4** was oxidized to the cationic complex **8** (Table 3). This suggests that the oxidation of the complex mainly occurs at N1 with some delocalization of the positive charge on the cobalt center. Consequently, the electronic structure of complex **3** was investigated in detail.

Table 3. Selected bond length [Å] and angles [°] for **1**, **2c**, **3–5**, and **8**.[27]

	1,[a] [Co(trop$_2$N)(bpy)] **2c**,[b] [Co(trop$_2$NH)(bpy)]PF$_6$ **3**, [Co(trop$_2$N)(bpy)]PF$_6$	**4**, [Rh(trop$_2$N)(bpy)] **5**, [Rh(trop$_2$NH)(bpy)]OTf **8**, [Rh(trop$_2$N)(bpy)]OTf
M—N1	1.954(2)	2.045(3)
	2.004(3)	2.090(2)
	1.842(2)	1.936(3)
M—N2	2.004(3)	2.152(3)
	2.030(3)	2.184(2)
	2.025(2)	2.175(3)
M—N3	1.991(2)	2.101(3)
	1.944(3)	2.049(2)
	1.991(2)	2.079(3)
M—ct1[c]	1.921(3)	2.017(4)
	1.946(3)	2.032(2)
	2.004(2)	2.073(4)
M—ct2[c]	1.923(3)	2.017(4)
	1.953(3)	2.055(2)
	1.983(2)	2.070(4)
C4—C5	1.429(4)	1.427(6)
	1.411(5)	1.436(3)
	1.401(3)	1.415(6)
C19—C20	1.416(4)	1.422(6)
	1.420(5)	1.417(3)
	1.404(3)	1.406(5)
N1-M-N3	171.7(1)	170.7(1)
	175.2(1)	174.1(1)
	178.7(1)	178.7(2)
ct1-M-ct2[c]	135.6(1)	134.2(1)
	135.4(2)	134.3(2)
	143.0(2)	143.9(2)
N1-M-N2	91.6(1)	93.4(1)
	94.5(1)	96.2(1)
	98.8(2)	102.1(2)
Σ° N1	343.6(2)	341.5(2)
	347.0(2)	345.1(1)
	358.4(3)	359.0(3)

[a] Two independent molecules per unit cell were found. The values reported correspond to the average. [b] Three independent molecules per unit cell were found. The values reported correspond to the average. [c] ct is the centroid of the coordinated C4=C5 and C19=C20 bonds.

Figure 4. ORTEP drawing of the molecular structure of **2c**. Thermal ellipsoids are drawn at 50% probability level. The counter anion PF$_6^-$, a solvate molecule of DME and all hydrogen atoms except at N1 are omitted for clarity; ct is the centroid of the coordinated C4=C5 and C19=C20 bonds, respectively. Three independent molecules per unit cell were found. The values reported for selected bond distances and angles correspond to the average. Selected bond distances [Å] and angles [°]: Co—N1 2.004(3), Co—N2 2.030(3), Co—N3 1.944(3), C4—C5 1.411(5), C19—C20 1.420(5), Co—ct1 1.946(3), Co—ct2 1.953(3); N1-Co-N3 175.2(1), ct1-Co-ct2 135.4(2), N1-Co-N2 94.5(1); Σ° N1 347.0(2).
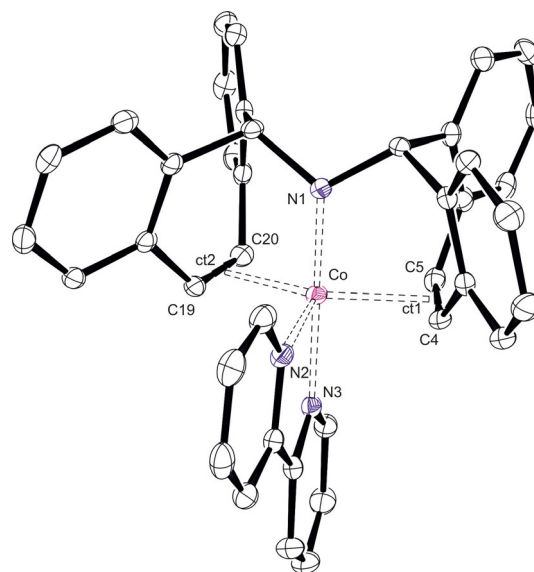
Figure 5. ORTEP drawing of the molecular structure of **3**. Thermal ellipsoids are drawn at 50% probability level. The counter anion PF$_6^-$ and all hydrogen atoms are omitted for clarity. ct is the centroid of the coordinated C4=C5 and C19=C20 bonds, respectively. Selected bond distances [Å] and angles [°]: Co—N1 1.842(2), Co—N2 2.025(2), Co—N3 1.991(2), C4—C5 1.401(3), C19—C20 1.404(3), Co—ct1 2.004(2), Co—ct2 1.983(2); N1-Co-N3 178.7(1), ct1-Co-ct2 143.0(2), N1-Co-N2 98.8(2); Σ° N1 358.4(3).

The electronic structure of **3** was studied by continuous wave (CW) EPR. The spectrum was recorded in frozen THF/toluene solution (120 K) (Figure 6). The *g*-values and anisotropic hyperfine coupling constants are listed in Table 4, and were obtained through simulation. Calculated values using DFT are also shown. The EPR spectrum of [Co(trop$_2$N)(bpy)](PF$_6$) (**3**) (Figure 6) reveals a rhombic spectrum, which is dominated by well-resolved cobalt hyperfine couplings along g_z. Additional hyperfine splitting with cobalt ($A^{Co}_x = A^{Co}_y = 50$ MHz), and a nitrogen atom ($A^N_y = 76$ MHz) are visible, but these splittings are rather poorly resolved in the experimental spectrum and consequently, their exact values from the simulation are not very reliable. Nonetheless, the DFT calculated EPR parameters of [Co(trop$_2$N)(bpy)]$^+$ correspond well with the experimental values (Table 4). A plot of the spin density distribution is displayed in Figure 7. Based on the calculations, the spin density of complex [Co(trop$_2$N)(bpy)]$^+$ is strongly delocalized over the metal and the amido functionality of the Ntrop$_2$ unit, with nearly equal spin densities at these atoms (Figure 7, Table 4). Th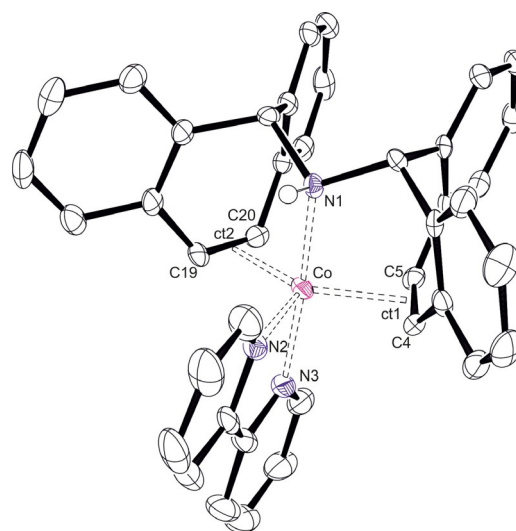e electronic structure is best described as a mixture between the Co^{II} amido and the Co^I aminyl radical form, which are, in this case, not discrete electromers but rather two limiting resonance structures contributing to the ground state of [Co(trop$_2$N)(bpy)]$^+$. The nitrogen atom (55%) has a slightly higher spin population than the cobalt center (47%), and

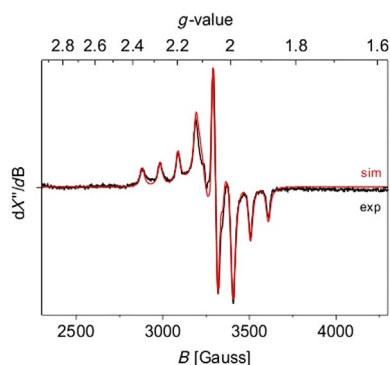**Figure 6.** Experimental and simulated X-band EPR spectrum of **3**, [Co(trop$_2$N)(bpy)]PF$_6$, in a frozen toluene/THF mixture measured at 120 K. Frequency 9.4920 GHz; microwave power 2 mW; modulation amplitude 1 G. Simulation: red, experimental: black.
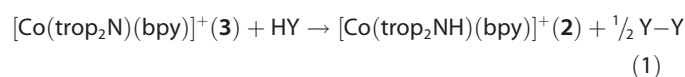
Table 4. Experimental[a] and DFT-calculated[b,c] EPR parameters of **3**.

g-tensor		g_z	g_x	g_y	
	Exptl	2.089	2.057	2.050	
	DFT[b]	*2.095*	*2.068*	*2.023*	
	DFT[c]	2.085	2.048	2.022	
A-tensor[d]		A_x	A_y	A_z	Spin density[e] [%]
Cobalt	Exptl	303	50 (PR)	50 (PR)	
^{59}Co	DFT[b]	*265*	*52*	*−49*	*51*
(*I*=7/2)	DFT[c]	−223	−45	49	47
N$_{aminyl\ radical}$	Exptl	NR	76 (PR)	NR	
^{14}N (*I*=1)	DFT[b]	*−1*	*75*	*−1*	*55*
	DFT[c]	−1	70	−1	51

[a] Spectral simulation; see Figure 6. [b] Orca, B3LYP, TZVP. [c] ADF, BP86, TZP. [d] Hyperfine couplings in MHz. [e] Mulliken atomic spin density. NR = not resolved; PR = poorly resolved.

Figure 7. Spin density plot of [Co(trop$_2$N)(bpy)]$^+$.

Table 5. Substrates H—Y used in the H-atom transfer reaction. The bond dissociation energies (BDEs) are given in kJ mol^{-1}. All reactions were carried out at room temperature in THF.[a]

Entry	H—X	BDE (H—Y) [kJ mol^{-1}]	Reaction (time)	Product	For **8** reaction/ product
1	*n*Bu$_3$SnH	310[37]	no	no	yes/ (*n*Bu$_3$Sn)$_2$
2	*n*BuSH	364[37]	yes (minutes)	(*n*BuS)$_2$	yes/(*t*BuS)$_2$[b]
3	Ph$_3$SiH	371[37]	no	no	no
4	Ph$_3$CH	339[38]	no	no	no
5	BHT[c]	340[39]	no	no	no[d]
6	TEMPOL[e]	289[40]	yes (2.5 h)	TEMPO[f]	–
7	Ph$_2$PH	376[37]	yes (4 h)	(Ph$_2$P)$_2$	–

[a] Conditions: [Co(trop$_2$N)(bpy)]PF$_6$ (18.0 mg, 24 μmol), XH (26 μmol), THF (1 mL), RT. [b] *t*BuSH was used instead of *n*BuSH. [c] BHT: 3,5-di-tertbutyl-4-hydroxytoluene. [d] Phenol was used instead of BHT. [e] TEMPOL: 2,2,6,6-tetramethylpiperidine-1-ol. [f] TEMPO: 2,2,6,6-tetramethylpiperidine-1-oxyl.

hence, the Co^I-aminyl radical description slightly prevails over the Co^{II}-amido. In the homologous complexes [Rh(trop$_2$N)(bpy)]$^+$ (**8**) and [Ir(trop$_2$N)(phen)]$^+$ (**9**), the spin density is more localized on N1 (computed spin populations: 60% on N1 and 30% on the metal center, the spin distribution being almost the same for **8** and **9**),[27, 30] Hence, in the complexes with the heavier metals, the aminyl radical character is more pronounced than for cobalt.

A typical reaction of radicals is H-atom transfer (HAT). In this sense, the reactivity of **3** toward substrates with different hydrogen atom donor abilities was investigated [Eq. (1) and Table 5].

$$[Co(trop_2N)(bpy)]^+ (\mathbf{3}) + HY \rightarrow [Co(trop_2NH)(bpy)]^+ (\mathbf{2}) + \tfrac{1}{2}\, Y{-}Y \tag{1}$$

The complex [Co(trop$_2$N)(bpy)]PF$_6$ (**3**) reacted rapidly with *n*BuSH to give an orange solution from which **2c** (NMR) and (*n*BuS)$_2$ (GC-MS) were identified (entry 2). The compound 2,2,6,6-tetramethylpiperidine-1-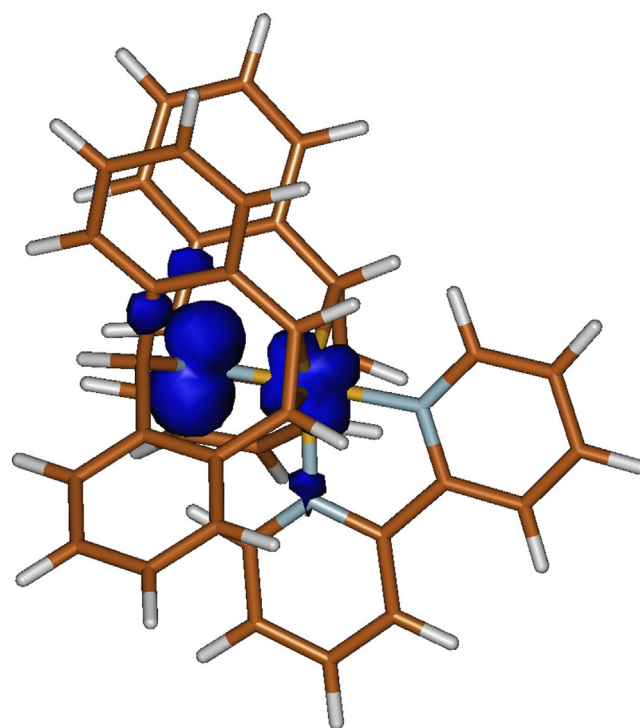ol reacted with **3** to yield complex **2c** and the radical 2,2,6,6-tetramethylpiperidine-1-oxyl (EPR, *g*-factor 2.006[33]) (Table 5, entry 6). With the secondary phosphine, PPh$_2$H, the reaction was slow and the formation of Ph$_2$P—PPh$_2$ was confirmed by ^{31}P{^{1}H} NMR (entry 7). No hydrogen atom abstraction was observed from Sn—H, Si—H, C—H, and O—H bonds in the compounds listed in Table 5 (entries 1, 3–5). For the heavier analogues [Rh(trop$_2$N)(bpy)]$^+$ (**8**)[27] and [Ir(trop$_2$N)(phen)]$^+$ (**9**),[30] a rapid and quantitative HAT was observed for substrates with bond dissociation energies (BDEs) lower than 360–350 kJ mol^{-1} (*n*Bu$_3$SnH and *n*BuSH). In those cases, the reactivity relates with the BDE of the N—H moiety in

the corresponding complexes [Rh(trop$_2$NH)(bpy)]$^+$ (**5**, 361 kJ mol^{-1}) and [Ir(trop$_2$NH)(phen)]$^+$ (**7**, 353 kJ mol^{-1}). The complex [Co(trop$_2$N)(bpy)]PF$_6$ (**3**) reacts only with the substrates with the lowest BDEs listed in Table 5 (289 kJ mol^{-1}). No reaction was observed between **3** and *n*BuSnH (310 kJ mol^{-1}) and this lack of reactivity, in marked contrast to the reactions reported for [Rh(trop$_2$N)(bpy)]$^+$ (**8**)[27] and [Ir(trop$_2$N)(phen)]$^+$ (**9**),[30] seems consistent with a slightly lower aminyl radical character of **3** as compared to its heavier metal analogues. Arguing purely on the basis of thermodynamic considerations,[34] the data point to a smaller BDE of the N–H bond in the cobalt amine complex than in the Rh and Ir analogs. Combined with a lower acidity of the cobalt amine complex relative to its heavier congeners, this could be a result of the lower reduction potential (Table 2) of the cobalt aminyl radical complex (BDFE ≈ 1.37pK_a + 23.06E^0 + 71.1).[35] However, the lack of reactivity of **3** with *n*BuSnH could also be for kinetic reasons.[36] Regardless of kinetic or thermodynamic arguments, the reduced HAT reactivity of the cobalt aminyl radical species seems in line with the smaller nitrogen atom spin population as compared to its heavier congeners.

Conclusions

The synthesis and characterization of three penta-coordinated cobalt complexes bearing the chelates trop$_2$NH and bpy has been described. These species [Co(trop$_2$N)(bpy)] (**1**), [Co(trop$_2$NH)(bpy)]PF6 (**2c**), and [Co(trop$_2$N)(bpy)]PF6 (**3**) are related to one another by either one-electron oxidation/reduction and/or transfer of a proton. Two limiting resonance structures can be used to describe the electronic structure of paramagnetic complex **3**: a cobalt(I)-aminyl radical and a cobalt(II)-amido complex. Structural analysis, EPR spectroscopy together with DFT calculations (hyperfine couplings and spin density), and hydrogen atom abstraction reactivity indicate that the cobalt(I)-aminyl radical character slightly prevails over the cobalt(II)-amido description. Upon comparing [Co(trop$_2$N)(bpy)]PF6 (**3**) with its heavier metal analogues [Rh(trop$_2$N)(bpy)]OTf (**8**) and [Ir(trop2NH)(phen)]PF6 (**9**), we can conclude that although their solid state structures are very similar, the complexes differ slightly in their electronic structure, with the aminyl radical character of the Rh and Ir species being higher than in the Co species. This is reflected in a lower propensity for HAT from Y–H donors of the Co-aminyl radical moiety.

Experimental Section

Synthesis and characterization

Preparation of [Co(trop$_2$N)(bpy)]·THF (1): [Co(HMDS)$_2$] (190.0 mg, 0.50 mmol), trop$_2$NH (216.8 mg, 0.55 mmol), 2,2′-bipyridine (82.1 mg, 0.53 mmol), and Zn powder (982.0 mg, 15.00 mmol) were combined in a Schlenk. Dry and degassed THF (3 mL) was added and the mixture was stirred at room temperature overnight. The dark suspension was filtered and layered with *n*-hexane (10 mL). Dark crystals were obtained, which were washed with *n*-hexane (3×3 mL) and dried under an Ar stream. Yield: 240.0 mg, 70%, air

sensitive; ^{1}H NMR (500.2 MHz, [D$_8$]THF): δ = 8.34 (d, $^3J_{HH}$ = 5.2 Hz, 1 H, CH^{ar}), 8.25 (d, $^3J_{HH}$ = 4.7 Hz, 1 H, CH^{ar}), 8.20 (d, $^3J_{HH}$ = 8.0 Hz, 1 H, CH^{ar}), 8.15 (d, $^3J_{HH}$ = 7.9 Hz, 1 H, CH^{ar}), 7.87 (td, $^3J_{HH}$ = 7.6 Hz, $^4J_{HH}$ = 1.5 Hz, 1 H, CH^{ar}), 7.63 (td, $^3J_{HH}$ = 7.6 Hz, $^4J_{HH}$ = 1.5 Hz, 1 H, CH^{ar}), 7.39 (t, $^3J_{HH}$ = 6.4 Hz, 1 H, CH^{ar}), 7.08–7.07 (m, 2 H, CH^{ar}), 6.92 (d, $^3J_{HH}$ = 7.4 Hz, 2 H, CH^{ar}), 6.82 (t, $^3J_{HH}$ = 6.4 Hz, 1 H, CH^{ar}), 6.78–6.75 (m, 2 H, CH^{ar}), 6.60–6.58 (m, 8 H, CH^{ar}), 6.52–6.51 (m, 2 H, CH^{ar}), 5.38 (d, $^3J_{HH}$ = 9.4 Hz, 2 H, CH^{olef}), 3.96 (d, $^3J_{HH}$ = 9.4 Hz, 2 H, CH^{olef}), 3.61 (m, 4 H, CH_2 from THF solvate), 3.04 (s, 2 H, CH^{benzyl}), 1.77 ppm (m, 4 H, CH_2 from THF solvate); ^{13}C{^{1}H} NMR (125.8 MHz, [D$_8$]THF): δ = 155.9 (s, C^{quat}), 153.5 (s, C^{quat}), 151.6 (s, CH^{ar}), 149.3 (s, CH^{ar}), 143.3 (s, C^{quat}), 142.5 (s, C^{quat}), 140.6 (s, C^{quat}), 138.5 (s, C^{quat}), 136.5 (s, CH^{ar}), 134.9 (s, CH^{ar}), 127.3 (s, CH^{ar}), 126.7 (s, CH^{ar}), 126.2 (s, CH^{ar}), 126.1 (s, CH^{ar}), 126.0 (s, CH^{ar}), 125.9 (s, CH^{ar})„ 125.6 (s, CH^{ar}), 124.3 (s, CH^{ar}), 123.9 (s, CH^{ar}), 123.3 (s, CH^{ar}), 121.5 (s, CH^{ar}), 120.5 (s, CH^{ar}), 79.4 (s, CH^{benzyl}), 73.5 (s, CH^{olef}), 71.2 (s, CH^{olef}), 68.0 (s, CH_2, THF solvate), 26.2 ppm (s, CH_2, THF solvate); ATR IR: $\tilde{v}$ = 3058 *w*, 3036 w, 3002 *m*, 2972 *m*, 2847 *m*, 1900 *w*, 1594 *m*, 1576 *m*, 1484 *s*, 1465 *s*, 1441 *s*, 1417 *m*, 1398 *m*, 1300 *m*, 1264 *s*, 1246 *s*, 1211 *s*, 1155 *s*, 1124 *s*, 1068 *s*, 1046 *s*, 1028 *s*, 989 *s*, 908 *m*, 882 *m*, 837 *m*, 823 *m*, 761 *s*, 739 *vs.*, 733 *vs.*, 704 *s*, 661 *m*, 645 *m*, 620 *w* cm^{-1}; elemental analysis calcd for C$_{40}$H$_{30}$CoN$_3$·C$_4$H$_8$O, C 77.29, H 5.60, N 6.15; found: C 77.60, H 5.78, N 6.18; HRMS (ESI): *m/z* calcd for C$_{40}$H$_{31}$CoN$_3$ 612.1844 [*M*+H]$^+$; found: 612.1860.

Preparation of [Co(trop$_2$NH)(bpy)][OTf] (2a), [Co(trop$_2$NH)(bpy)][BAr$^F_4$] (2b), and [Co(trop$_2$NH)(bpy)][PF$_6$] (2c): Bromoacetic acid (14.0 mg, 0.10 mmol) dissolved in THF (1 mL) was added dropwise to a stirred solution of [Co(trop$_2$N)(bpy)]·THF (68.4 mg, 0.10 mmol) in THF (2 mL). An orange suspension was obtained rapidly, which was stirred at room temperature for 4 h. The solvent was decanted and the solid was washed with diethyl ether (3×3 mL). Yield 69.1 mg, 92% as orange solid. The obtained [Co(trop$_2$NH)(bpy)][O$_2$CH$_2$Br] (52.5 mg, 70 μmol) was suspended in THF (3 mL) and NaOTf (13.1 mg, 76 μmol), NaBAr$^F_4$ (64.7 mg, 73 μmol), or KPF$_6$ (13.4 mg, 73 μmol) was added accordingly. The mixture was stirred overnight at room temperature. After filtration, the orange-reddish clear filtrate was layered with *n*-hexane (10 mL). Yield: 35.0 mg, 60% (**2a**); 86.0 mg, 79% (**2b**); 31.8 mg, 60% (**2c**). [Co(trop$_2$NH)(bpy)]PF$_6$ (**2c**) was also prepared by addition of 2,2,6,6-tetramethylpiperidine-1-ol (4.1 mg, 26 μmol) or Ph$_2$PH (4.9 mg, 26 μmol) to a solution of [Co(trop$_2$N)(bpy)]PF$_6$ (18.0 mg, 24 μmol) in THF (1 mL). The orange-reddish solution was layered with diethyl ether (4 mL). The complex **2c** was isolated as an orange solid. Yield: 16.0 mg, 89%.

[Co(trop$_2$NH)(bpy)][OTf] (2a): ^{1}H NMR (500.2 MHz, [D$_8$]THF): δ = 8.63 (d, $^3J_{HH}$ = 7.9 Hz, 1 H, CH^{ar}), 8.45 (d, $^3J_{HH}$ = 5.5 Hz, 1 H, CH^{ar}), 8.42 (d, $^3J_{HH}$ = 7.9 Hz, 1 H, CH^{ar}), 7.98 (td, $^3J_{HH}$ = 7.2 Hz, $^4J_{HH}$ = 3.2 Hz, 2 H, CH^{ar}), 7.55 (t, $^3J_{HH}$ = 6.1 Hz, 1 H, CH^{ar}), 7.49–7.48 (m, 3 H, CH^{ar}), 7.35 (d, $^3J_{HH}$ = 7.4 Hz, 2 H, CH^{ar}), 7.20 (t, $^3J_{HH}$ = 6.1 Hz, 1 H, CH^{ar}), 7.00 (td, $^3J_{HH}$ = 7.4 Hz, $^4J_{HH}$ = 1.0 Hz, 2 H, CH^{ar}), 6.93–6.85 (m, 10 H, CH^{ar}), 6.21 (d, $^3J_{HH}$ = 9.5 Hz, 2 H, CH^{olef}), 4.79 (d, $^3J_{HH}$ = 9.5 Hz, 2 H, CH^{olef}), 4.34 (s, 2 H, CH^{benzyl}), 0.86 ppm (br, 1 H, NH); ^{13}C{^{1}H} NMR (125.8 MHz, [D$_8$]THF): δ = 156.0 (s, C^{quat}), 155.0 (s, C^{quat}), 151.7 (s, CH^{ar}), 149.2 (s, CH^{ar}), 138.8 (s, CH^{ar}), 138.0 (s, CH^{ar}), 136.7 (q, $^1J_{FC}$ = 244.7 Hz, CF_3), 129.7 (s, CH^{ar}), 129.3 (s, CH^{ar}), 129.2 (s, CH^{ar}), 128.7 (s, CH^{ar}), 127.9 (s, CH^{ar}), 127.6 (s, C^{quat}), 127.5 (s, CH^{ar}), 127.4 (s, C^{quat}), 126.3 (s, CH^{ar}), 125.5 (s, CH^{ar}), 123.9 (s, CH^{ar}), 123.2 (s, CH^{ar}), 75.7 (s, CH^{olef}), 75.6 (s, CH^{olef}), 70.6 ppm (s, CH^{benzyl}); ^{19}F{^{1}H} NMR (188.3 MHz, [D$_8$]THF): δ = −78.79 ppm (s); elemental analysis calcd for C$_{41}$H$_{31}$CoF$_3$N$_3$O$_3$S·0.5C$_4$H$_8$O, C 64.74, H 4.42, N 5.27; found for: C 64.45, H 4.57, N 5.27. MS (MALDI-TOF): *m/z* calcd for C$_{40}$H$_{31}$CoN$_3$ 612.1844 [*M*]$^+$; found: 612.1836; air sensitive.

[Co(trop₂NH)(bpy)][BArᶠ₄] (2 b): ¹H NMR (500.2 MHz, [D₈]THF): $\delta =$ 8.59 (d, $^3J_{HH} = 7.8$ Hz, 1 H, CH^{ar}), 8.41 (d, $^3J_{HH} = 4.9$ Hz, 1 H, CH^{ar}), 8.32 (d, $^3J_{HH} = 7.7$ Hz, 1 H, CH^{ar}), 8.14 (m, 1 H, CH^{ar}), 8.02 (t, $^3J_{HH} = 7.4$ Hz, 1 H, CH^{ar}), 7.80 (m, 8 H, CH^{ar}), 7.58 (m, 3 H, CH^{ar}), 7.51 (t, $^3J_{HH} = 6.2$ Hz, 1 H, CH^{ar}), 7.46 (d, $^3J_{HH} = 6.0$ Hz, 2 H, CH^{ar}), 7.28 (m, 3 H, CH^{ar}), 7.11 (m, 4 H, CH^{ar}), 7.06–7.02 (m, 4 H, CH^{ar}), 6.95 (m, 4 H, CH^{ar}), 6.75 (d, $^3J_{HH} = 5.6$ Hz, 2 H, CH^{ar}), 6.25 (d, $^3J_{HH} = 9.4$ Hz, 2 H, CH^{olef}), 4.91 (d, $^3J_{HH} = 9.5$ Hz, 2 H, CH^{olef}), 4.02 (s, 2 H, CH^{benzyl}), 0.43 ppm (br, 1 H, NH); ¹⁹F{¹H} NMR (188.3 MHz, [D₈]THF): $\delta = -62.27$ ppm (s); ATR IR: $\tilde{\nu} = 3074$ w, 3022 w, 2976 br, 2870 br, 1607 m, 1478 m, 1444 w, 1353 s, 1272 $vs.$, 1156 s, 1114 br and $vs.$, 886 s, 838 s, 752 br and s, 710 s, 681 s, 668 s, 617 w cm⁻¹; air sensitive.

[Co(trop₂NH)(bpy)][PF₆] (2 c): ¹H NMR (500.2 MHz, [D₈]THF): $\delta =$ 8.69 (d, $^3J_{HH} = 8.1$ Hz, 1 H, CH^{ar}), 8.56 (d, $^3J_{HH} = 5.9$ Hz, 1 H, CH^{ar}), 8.45 (d, $^3J_{HH} = 8.2$ Hz, 1 H, CH^{ar}), 8.17–8.03 (m, 1 H, CH^{ar}), 7.82–6.75 (m, 20 H, CH^{ar}), 6.37 (d, $^3J_{HH} = 9.5$ Hz, 2 H, CH^{olef}), 4.95 (d, $^3J_{HH} = 9.3$ Hz, 2 H, CH^{olef}), 4.51 (s, 2 H, CH^{benzyl}), 0.58 ppm (br, 1 H, NH); ¹³C{¹H} NMR (125.8 MHz, [D₈]THF): $\delta = 154.9$ (s, C^{quat}), 151.2 (s, C^{quat}), 147.4 (s, CH^{ar}), 138.9 (s, CH^{ar}), 138.2 (s, CH^{ar}), 137.6 (s, CH^{ar}), 136.8 (s, CH^{ar}), 130.5 (s, CH^{ar}), 130.4 (s, CH^{ar}), 129.9 (s, CH^{ar}), 129.4 (s, CH^{ar}), 128.6 (s, CH^{ar}), 127.9 (s, C^{quat}), 127.3 (s, CH^{ar}), 127.2 (s, C^{quat}), 126.9 (s, CH^{ar}), 125.5 (s, CH^{ar}), 124.8 (s, CH^{ar}), 123.3 (s, CH^{ar}), 75.1 (s, CH^{olef}), 74.9 (s, CH^{olef}), 69.8 ppm (s, CH^{benzyl}); ¹⁹F{¹H} NMR (188.3 MHz, [D₈]THF): $\delta = -72.7$ ppm (d, $^1J_{PF} = 708.0$ Hz); ³¹P{¹H} NMR (202.5 MHz, [D₈]THF): $\delta = -142.8$ ppm (m, $^1J_{PF} = 708.0$ Hz); air sensitive.

Preparation of [Co(trop₂N)(bpy)]PF₆ (3): [Co(trop₂N)(bpy)]·THF (**1**) (160.0 mg, 0.23 mmol) and [FeCp₂]PF₆ (80.6 mg, 0.24 mmol) were combined in a Schlenk. Dry and degassed toluene (3 mL) was added and the mixture was stirred at room temperature, overnight. A pale-green precipitate was formed. The solvent was decanted and the product was washed with toluene (2×2 mL) and n-hexane (3×3 mL). The obtained green powder was dried under vacuum. Single crystals suitable for X-ray analysis were obtained from CH₂Cl₂/n-hexane mixtures. Yield: 80.0 mg, >99%. MS (MALDI-TOF): m/z calcd for C₄₀H₃₀CoN₃ 611.177 [M]⁺; found: 612.013. $\mu_{eff,1} =$ 1.9 μ_B (2–105 K) and $\mu_{eff,2} = 2.4$ μ_B. (29–100 K); EPR (X-band, 9.49 GHz, toluene/THF, 120 K): g-tensor M⁻ (2.089, 2.057, 2.050), ⁵⁹Co ($I = 7/2$) A-tensor M⁻ (303, 50, 50), ¹⁴N$_{aminyl}$ ($I = 1$) A-tensor M⁻ (not resolved, 76, not resolved); air sensitive.

Reactivity tests

[Co(trop₂N)(bpy)]PF₆ (18.0 mg, 24 μmol) and XH (26 μmol) were combined in a Schlenk flask (for the list of substrates, see Table 5). THF (1 mL) was added and the mixture was stirred at room temperature. The initial green suspension becomes a clear orange solution when the reaction takes place. An aliquot of the reaction mixture was taken, evaporated to dryness, and analyzed by ¹H NMR to confirm the formation of **2 c**. For the reaction with nBu₃SnH as H-donor, GC-MS analysis was performed to detect (nBu₃S)₂. For the reaction with 2,2,6,6-tetramethylpiperidine-1-ol, an EPR spectrum was recorded to identify the TEMPO radical. The reaction with Ph₂PH was followed by ³¹P{¹H} NMR.

Acknowledgements

Conflict of interest

The authors declare no conflict of interest.

[1] R. G. Hicks, *Angew. Chem. Int. Ed.* **2008**, *47*, 7393–7395; *Angew. Chem.* **2008**, *120*, 7503–7505.

[2] P. Chaudhuri, K. Wieghardt, in *Progess in Inorganic Chemistry, Vol. 50* (Ed.: K. D. Karlin), Wiley, Hoboken, **2001**, pp. 151–216.

[3] R. G. Hicks, *Aust. J. Chem.* **2001**, *54*, 597–600.

[4] K. E. Preuss, *Dalton Trans.* **2007**, 2357–2369.

[5] For a recent review on complexes with nitrogen-centered radical ligands, see: A. I. Olivos Suarez, V. Lyaskovskyy, J. N. H. Reek, I. J. I. van der Vlugt, B. de Bruin, *Angew. Chem. Int. Ed.* **2013**, *52*, 12510–12529; *Angew. Chem.* **2013**, *125*, 12740–12760.

[6] a) A. R. Forrester, A. M. Hay, R. H. Thomson, in *Organic Chemistry of Stable Free Radicals*, Academic Press, London, **1968**, p.111; b) G. Merényi, J. Lind, in *N-Centered Radicals* (Ed.: Z. B. Alfassi), Wiley, Hoboken, **1998**, pp. 599–613; c) B. J. Maxwell, J. Tsanaktsidis, in *N-Centered Radicals* (Ed.: Z. B. Alfassi), Wiley, Hoboken, **1998**, pp. 663–684.

[7] E. Kogut, H. L. Wiencko, L. Zhang, D. E. Cordeau, T. H. Warren, *J. Am. Chem. Soc.* **2005**, *127*, 11248–11249.

[8] For spectroscopic characterization of catalytically relevant imidyl/nitrene radical complexes of cobalt porphyrins, see: a) M. Goswami, V. Lyaskovskyy, S. R. Domingos, W. J. Buma, S. Woutersen, O. Troeppner, I. Ivanović-Burmazović, H. Lu, X. Cui, X. P. Zhang, E. J. Reijerse, S. DeBeer, M. M. van Schooneveld, F. F. Pfaff, K. Ray, B. de Bruin, *J. Am. Chem. Soc.* **2015**, *137*, 5468–5479; b) V. Lyaskovskyy, A. I. Olivos Suárez, H. Lu, H. Jiang, X. P. Zhang, B. de Bruin, *J. Am. Chem. Soc.* **2011**, *133*, 12264–12273.

[9] For the chromium species [(L₂Cr³⁺)(⁻NAd)]²⁺, in which L = 2,6-bis(1-methylethyl)-N-(2-pyridinylmethylene)phenylamine and Ad = 1-adamantyl, see: C. C. Lu, S. George, T. Weyhermüller, E. Bill, E. Bothe, K. Wieghardt, *Angew. Chem. Int. Ed.* **2008**, *47*, 6384–6387; *Angew. Chem.* **2008**, *120*, 6484–6487.

[10] For Ru and Os complexes of the type [(SiPiPr₃)M²⁺]⁺[NAr⁻], in which SiPiPr₃ = (2-iPr₂P-C₆H₄)₃Si⁻ and Ar = 4-CF₃-C₆H₄, see: A. Takaoka, L. C. H. Gerber, J. C. Peters, *Angew. Chem. Int. Ed.* **2010**, *49*, 4088–4091; *Angew. Chem.* **2010**, *122*, 4182–4185.

[11] For a complex with the general formula [(LFe³⁺)(⁻NAd)], in which L = 2,6-(2,6-iPr₂-C₆H₃-N = CMe)₂C₅H₃N and Ad = 1-adamantyl, see: A. C. Bowman, C. Milsmann, E. Bill, Z. R. Turner, E. Lobkovsky, S. DeBeer, K. Wieghardt, P. J. Chirik, *J. Am. Chem. Soc.* **2011**, *133*, 17353–17369.

[12] For a complex with the general formula [(L^{Me}Fe)⁺(⁻NAd)], in which L^{Me} = 2,4-bis(2,6-diisopropylphenylimido)pentyl and Ad = 1-adamantyl, see: a) R. E. Cowley, N. A. Eckert, S. Vaddadi, T. M. Figg, T. R. Cundari, P. L. Holland, *J. Am. Chem. Soc.* **2011**, *133*, 9796–9811; b) R. E. Cowley, N. J. DeYonker, N. A. Eckert, T. R. Cundari, S. DeBeer, E. Bill, X. Ottenwaelder, C. Flaschenriem, P. L. Holland, *Inorg. Chem.* **2010**, *49*, 6172–6187; c) N. A. Eckert, S. Vaddadi, S. Stoian, R. J. Lachicotte, T. R. Cundari, P. L. Holland, *Angew. Chem. Int. Ed.* **2006**, *45*, 6868–6871; *Angew. Chem.* **2006**, *118*, 7022–7025.

[13] For Ni, Fe and Ru imidyl complexes bearing a PNP ligand or pincer ligands, see: A. N. Walstrom, B. C. Fullmer, H. Fan, M. Pink, D. T. Buschhorn, K. G. Caulton, *Inorg. Chem.* **2008**, *47*, 9002–9009.

[14] a) For an iron species with the general formula [(^{Ar}LFeCl)⁺(⁻N(4-tBu-C₆H₄)], in which ^{Ar}L = 1,9-Ar₂-5-mesityl-dipyrromethene and Ar = 2,4,6-Ph₃-C₆H₂, see: E. R. King, E. T. Hennessy, T. A. Betley, *J. Am. Chem. Soc.* **2011**, *133*, 4917–4923; b) for the formation of a Fe^{III} imidyl radical as plausible intermediate in the catalytic intramolecular C—H amination of alkyl azides, see: E. T. Hennessy, T. A. Betley, *Science* **2013**, *340*, 591–595.

[15] Y. Miyazato, T. Wada, J. T. Muckerman, E. Fujita, K. Tanaka, *Angew. Chem. Int. Ed.* **2007**, *46*, 5728–5730; *Angew. Chem.* **2007**, *119*, 5830–5832.

[16] a) B. L. Tran, M. P. Washington, D. A. Henckel, X. Gao, H. Park, M. Pink, D. J. Mindiola, *Chem. Commun.* **2012**, *48*, 1529–1531; b) M. G. Scheibel, B. Askevold, F. W. Heinemann, E. J. Reijerse, B. de Bruin, S. Schneider,

Nat. Chem. **2012**, *4*, 552–558; c) M. G. Scheibel, J. Abbenseth, M. Kinauer, F. W. Heinemann, C. Würtele, B. de Bruin, S. Schneider, *Inorg. Chem.* **2015**, *54*, 9290–9302.

[17] M. G. Scheibel, Y. Wu, A. C. Stückl, L. Krause, E. Carl, D. Stalke, B. de Bruin, S. Schneider, *J. Am. Chem. Soc.* **2013**, *135*, 17719–17722.

[18] Y. Gloaguen, C. Rebreyend, M. Lutz, P. Kumar, M. Huber, I. J. I. van der V-lugt, S. Schneider, B. de Bruin, *Angew. Chem. Int. Ed.* **2014**, *53*, 6814–6818; *Angew. Chem.* **2014**, *126*, 6932–6936.

[19] a) D. Sellmann, J. Müller, P. Hofmann, *Angew. Chem. Int. Ed. Engl.* **1982**, *21*, 691–692; *Angew. Chem.* **1982**, *94*, 708–709; b) D. Sellmann, J. Müller, *J. Organomet. Chem.* **1985**, *281*, 249–262.

[20] a) R. Gross, W. Kaim, *Angew. Chem. Int. Ed. Engl.* **1985**, *24*, 856–858; *Angew. Chem.* **1985**, *97*, 869–870; b) R. Gross, W. Kaim, *Inorg. Chem.* **1987**, *26*, 3596–3600.

[21] D. Adhikari, S. Mossin, F. Basuli, J. C. Huffman, R. K. Szilagyi, K. Meyer, D. J. Mindiola, *J. Am. Chem. Soc.* **2008**, *130*, 3676–3682.

[22] A. T. Radosevich, J. G. Melnick, S. A. Stoian, D. Bacciu, C.-H. Chen, B. M. Foxman, O. V. Ozerov, D. G. Nocera, *Inorg. Chem.* **2009**, *48*, 9214–9221.

[23] S. B. Harkins, N. P. Mankad, A. J. M. Miller, R. K. Szilagyi, J. C. Peters, *J. Am. Chem. Soc.* **2008**, *130*, 3478–3485.

[24] N. P. Mankad, W. E. Antholine, R. K. Szilagyi, J. C. Peters, *J. Am. Chem. Soc.* **2009**, *131*, 3878–3880.

[25] M. M. Melzer, S. Mossin, X. Dai, A. M. Bartell, P. Kapoor, K. Meyer, T. H. Warren, *Angew. Chem. Int. Ed.* **2010**, *49*, 904–907; *Angew. Chem.* **2010**, *122*, 916–919.

[26] F. N. Penkert, T. Weyhermüller, E. Bill, P. Hildebrandt, S. Lecomte, K. Wieghardt, *J. Am. Chem. Soc.* **2000**, *122*, 9663–9673.

[27] T. Büttner, J. Geier, G. Frison, J. Harmer, C. Calle, A. Schweiger, H. Schönberg, H. Grützmacher, *Science* **2005**, *307*, 235–238.

[28] P. Maire, M. Königsmann, A. Sreekanth, J. Harmer, A. Schweiger, H. Grützmacher, *J. Am. Chem. Soc.* **2006**, *128*, 6578–6580.

[29] M. Königsmann, N. Donati, D. Stein, H. Schönberg, J. Harmer, A. Sreekanth, H. Grützmacher, *Angew. Chem. Int. Ed.* **2007**, *46*, 3567–3570; *Angew. Chem.* **2007**, *119*, 3637–3640.

[30] N. Donati, D. Stein, T. Büttner, H. Schönberg, J. Harmer, A. Sreekanth, H. Grützmacher, *Eur. J. Inorg. Chem.* **2008**, 4691–4703.

[31] A. J. Rosenthal, M. Vogt, B. de Bruin, H. Grützmacher, *Eur. J. Inorg. Chem.* **2013**, 5831–5835.

[32] S. Wiese, Y. M. Badiei, R. T. Gephart, S. Mossin, M. S. Varonka, M. M. Melzer, K. Meyer, T. R. Cundari, T. H. Warren, *Angew. Chem. Int. Ed.* **2010**, *49*, 8850–8855; *Angew. Chem.* **2010**, *122*, 9034–9039.

[33] a) V. Mugnaini, C. Punta, R. Liantonio, P. Metrangolo, F. Recupero, G. Resnati, G. F. Pedulli, M. Lucarini, *Tetrahedron Lett.* **2006**, *47*, 3265–3269; b) M. A. M. Noël, R. D. Allendoerfer, R. A. Osteryoung, *J. Phys. Chem.* **1992**, *96*, 2391–2394.

[34] J. M. Mayer, *Acc. Chem. Res.* **2011**, *44*, 36–46.

[35] J. J. Warren, T. A. Tronic, and J. M. Mayer, *Chem. Rev.* **2010**, *110*, 6961–7001.

[36] N. Dietl, M. Schlangen, H. Schwarz, *Angew. Chem. Int. Ed.* **2012**, *51*, 5544–5555; *Angew. Chem.* **2012**, *124*, 5638–5650.

[37] Experimental data was collected from: Y.-R. Luo, in *Handbook of Bond Dissociation Energies in Organic Compounds*, CRC, Florida, **2003**.

[38] F. G. Bordwell, J.-P. Cheng, G.-Z. Ji, A. V. Satish, X. Zhang, *J. Am. Chem. Soc.* **1991**, *113*, 9790–9795.

[39] M. Lucarini, G. F. Pedulli, L. Valgimigli, R. Amorati, *J. Org. Chem.* **2001**, *66*, 5456–5462.

[40] S. Wertz, A. Studer, *Green Chem.* **2013**, *15*, 3116–3134.